1. The PDF file of Supplemental Information includes 6 Figures, 3 Tables, and Supplemental Experimental Procedures.
2. Tables 1 and 3 are separate Excel files.

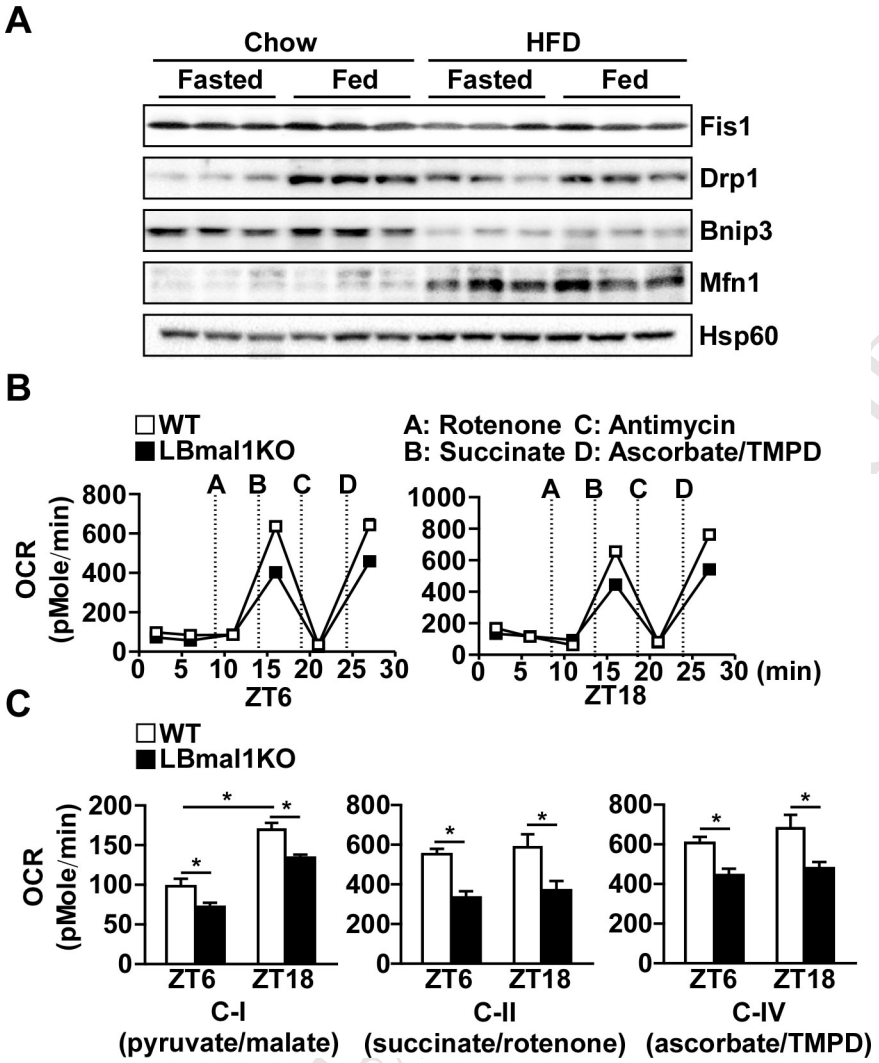

Figure S1 (related to Figure 1). Bmal1 regulates mitochondrial function

(A) Mitochondrial dynamics protein expression at fasted (ZT8) and fed (ZT20) states in the liver of mice under chow or high fat diet (HFD for 5 months, n=3/time point). (B) Mitochondrial electron flow determined by substrate driven mitochondrial respiration. The oxygen consumption rate (OCR) was determined in isolated mitochondria from WT and LBmal1KO livers at ZT6 or ZT18. Mitochondria were incubated in pyruvate/malate containing buffer before subjecting to sequential addition of rotenone, succinate, antimycin A and ascorbate/TMPD (referred by A-D). (C) Assessment of complex I (C-I), II, and IV respiration based on data in (B). Data presented as mean ± SEM. *p<0.05.

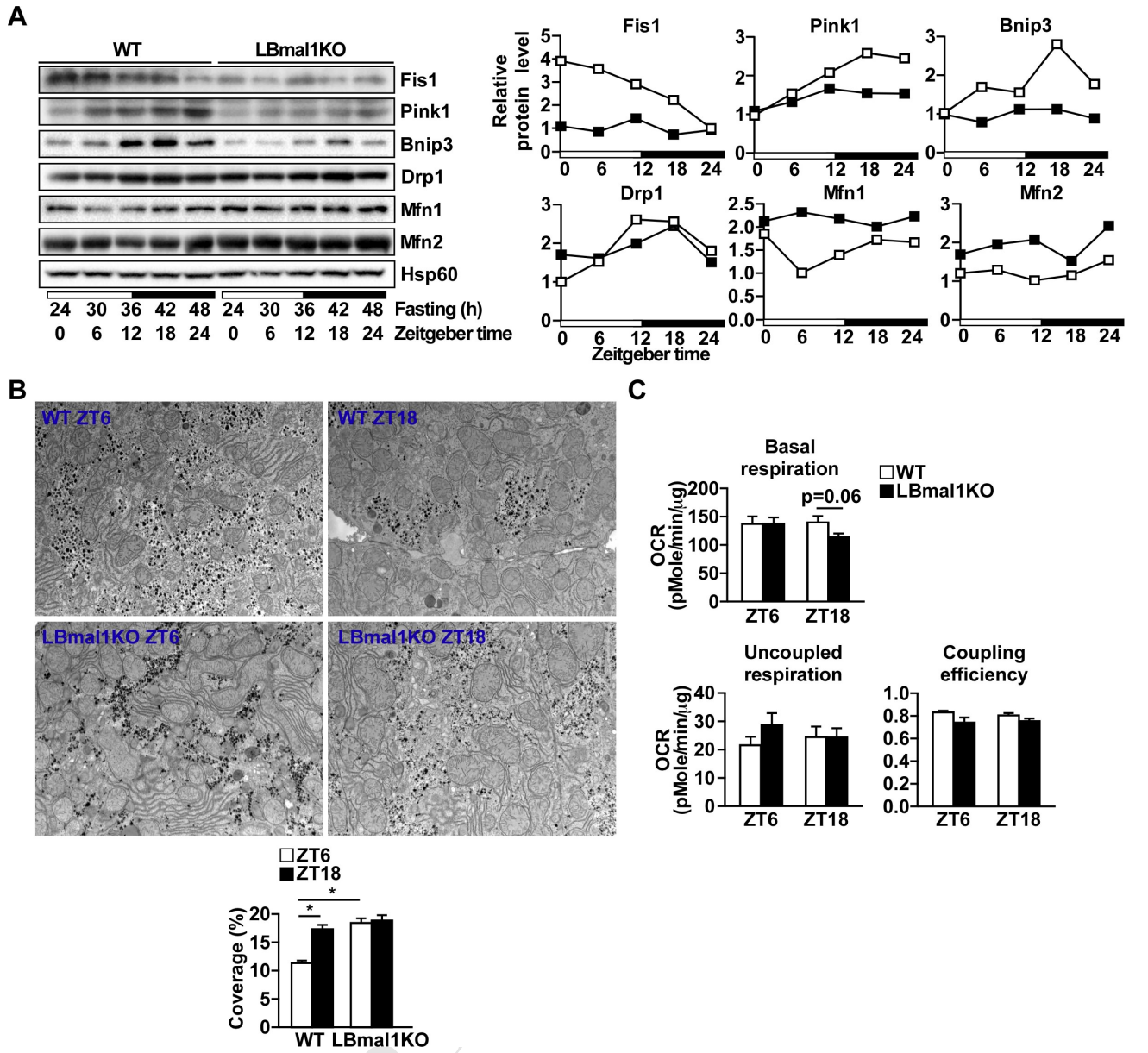

Figure S2 (related to Figure 2). Fasting has differential effects on mitochondrial morphology and respiration.

(A) Expression of mitochondrial dynamics protein in WT and LBmal1KO livers under constant fasting (n=3-4/time point/genotype). The white and black bar represents light cycle and dark cycle, respectively. Right panel: Quantification of the Western blot normalizing to Hsp60. (B) Representative electron microscopy images of liver sections from WT and LBmal1KO mice (n=3/time point/genotype) at ZT6 and ZT18 under constant fasting. Bottom panel: Mitochondrial coverage calculated from EM images in 1000 μm^2 surface area. (C) The basal oxygen consumption rate (OCR), uncoupled respiration, and coupling efficiency in primary hepatocytes isolated from WT and LBmal1KO mice at ZT6 and ZT18 under constant fasting. Data presented as mean ± SEM. *p<0.05.

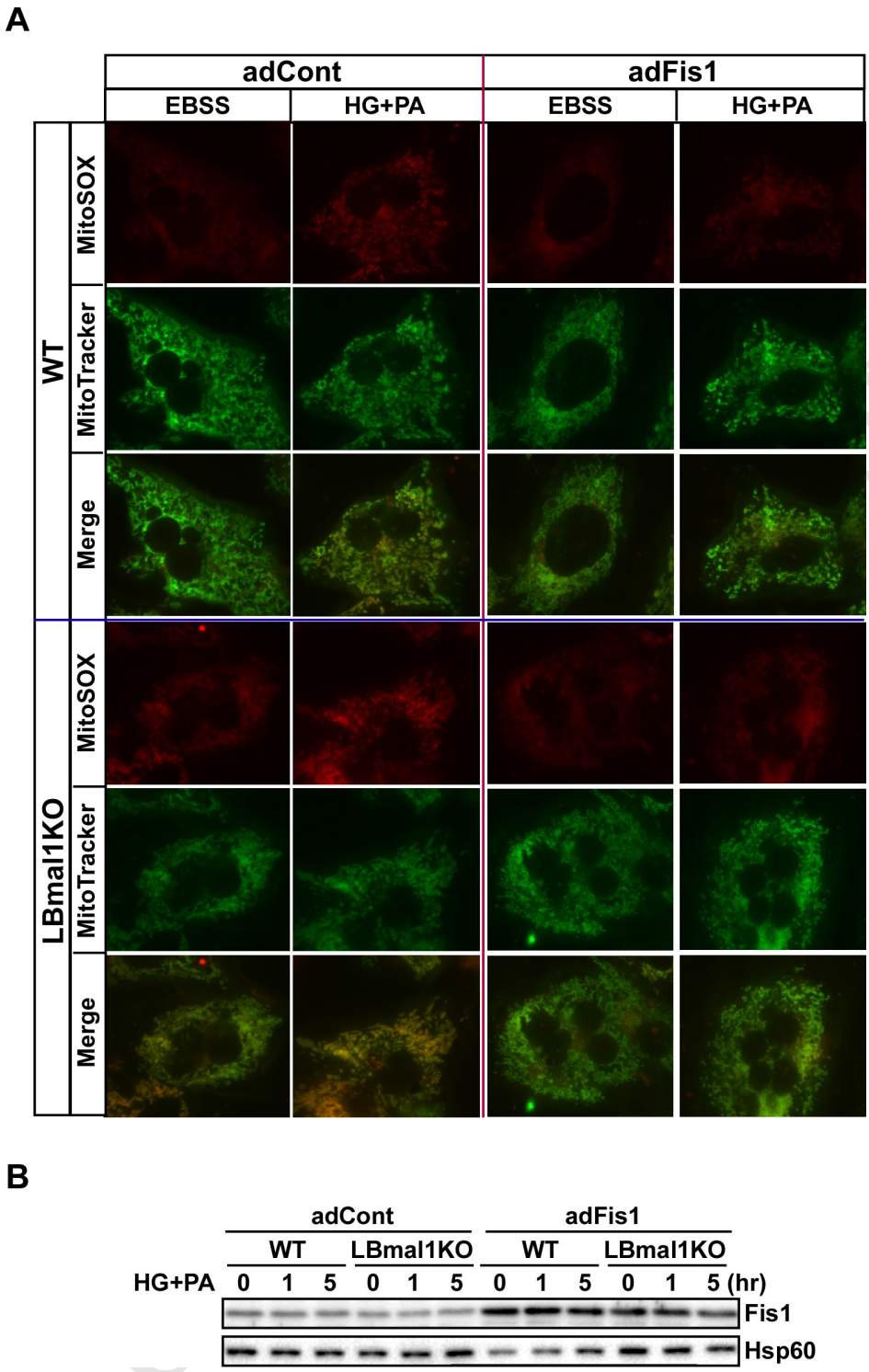

Figure S3 (related to Figure 4). Fis1 overexpression reduces oxidative stress in LBmal1KO hepatocytes
(A) Representative images demonstrating the assessment of mitochondrial ROS levels. Superoxide production was monitored by MitoSOX Red and mitochondrial mass by MitoTracker Green in WT and LBmal1KO primary hepatocytes. Hepatocytes were transduced with control virus (adCont) or adFis1 and cultured in EBSS or 25 mM glucose/0.3 mM palmitic acid (HG+PA) for 3 hours. (B) Western blotting showing Fis1 protein levels. Hepatocytes were in EBSS (HG+PA 0 hr) or in HG+PA for 1 or 5 hr.

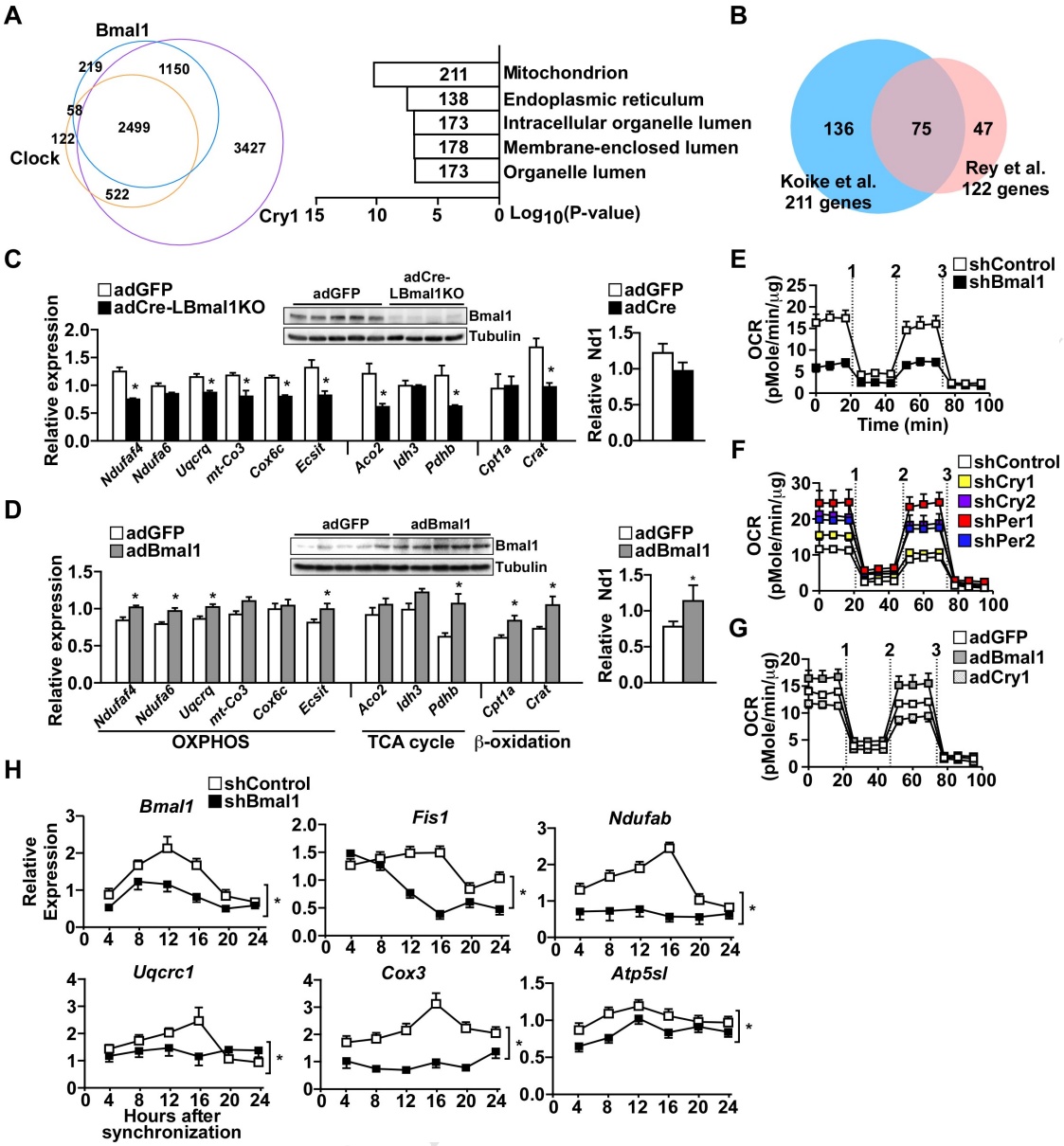

Figure S4 (related to Figure 5). Mitochondrial respiration is a common target of Bmal1, Clock, and Cry1

(A) Venn diagrams showing cross-comparison of Bmal1, Clock, and Cry1 bound genes based on published ChIP-seq dataset (Koike et al. 2012). Right: Gene ontology analysis of the commonly bound 2499 genes. The top 5 enriched cellular components based on nominal p values are presented. The number of genes in each ontology category is shown. (B) Cross-comparison of Bmal1/Clock/Cry1 bound genes identified by (Koike et al., 2012) (211 genes) or Bmal1 bound genes by (Rey et al., 2011) (122 genes) related to mitochondrial function. (C) Hepatic expression of Bmal1 target genes in oxidative metabolism quantified by real-time PCR in control (adGFP) versus acute *Bmal1* deletion (adCre-LBmal1KO). Liver samples from 2-month-old, chow-fed mice (n=4-5) were collected at ZT18 two weeks after tail vein injection of the adenoviral vectors. Bmal1 and tubulin (loading control) protein levels are shown. Right panel: mitochondrial DNA content determined by relative *Nd1* levels. (D) Hepatic expression of Bmal1 target genes (left panel) and mitochondrial DNA content (right panel) in control (adGFP) versus transient *Bmal1* over-expression (adBmal1) mice (n=5). (E) The oxygen consumption rate (OCR) in Hepa 1-6 cells with control (shControl) or stable *Bmal1* knockdown (shBmal1). (F) OCRs in Hepa 1-6 cells with stable *Cry1*, *Cry2*, *Per1*, or *Per2* knockdown. (G) OCRs in Hepa 1-6 cells with adenoviral mediated over-expression of *Bmal1* (adBmal1) or *Cry1* (adCry1). Numbers 1-3 refer to the time course of adding oligomycin, FCCP, and antimycin A/rotenone, respectively. (H) Expression of mitochondrial OXPHOS and dynamics genes in synchronized shControl and shBmal1 Hepa 1-6 cells. Data presented as mean ± SEM. *p<0.05.

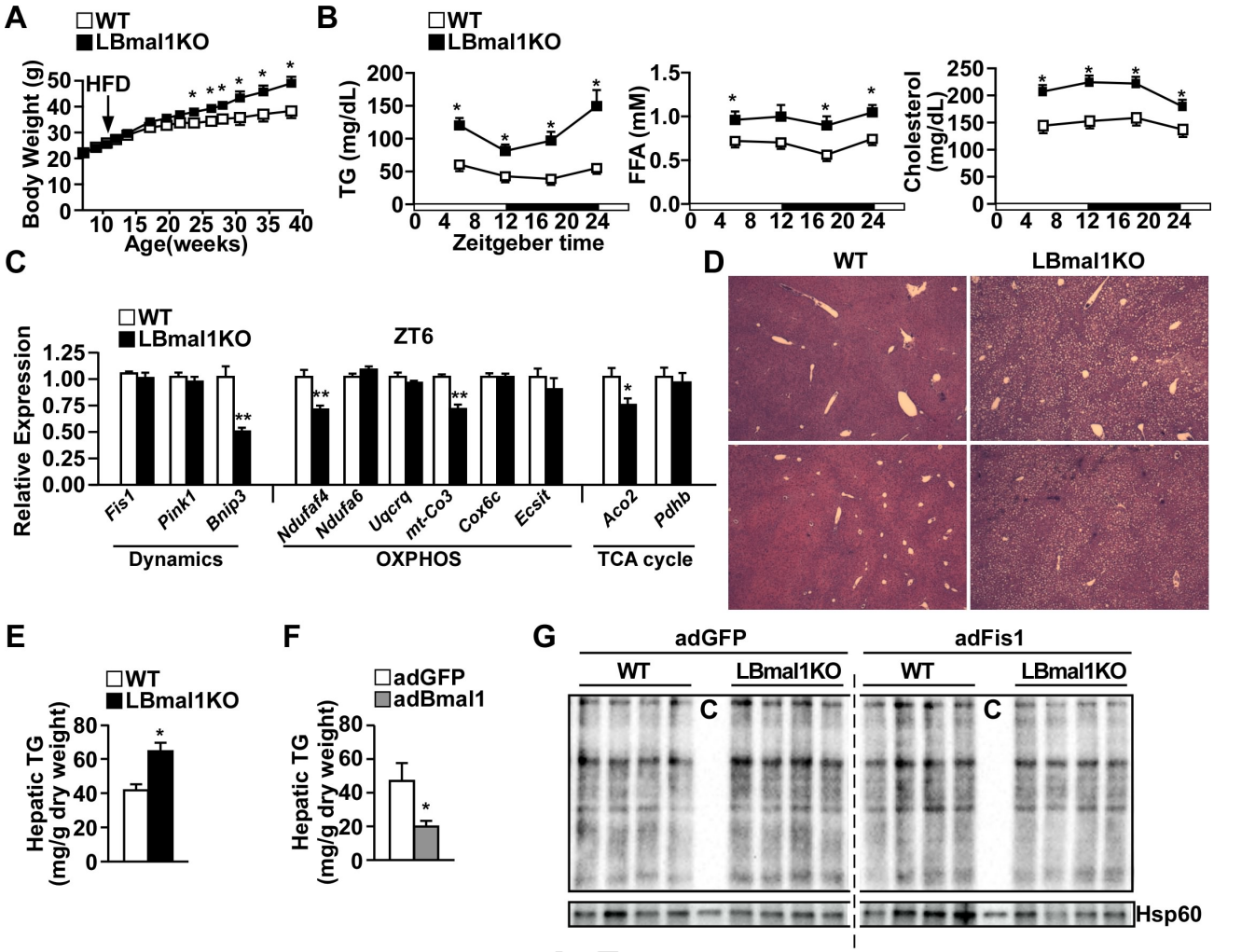

Figure S5 (related to Figure 6). LBmal1KO mice develop obesity, hyperlipidemia, and fatty liver

(A) Body weight in control and LBmal1KO mice (n=7-8/group). Arrow indicates the starting time of high fat diet (HFD) feeding. (B) *Ad libitum* serum triglycerides, free fatty acids, and cholesterol levels at different time of the day in control and LBmal1KO mice (2 months on HFD). (C) Expression of Bmal1 targets involved in mitochondrial function in liver from WT and LBmal1KO mice on high fat diet (HFD) for 5 months. Samples were collected at ZT6 (n=7-8/genotype). (D) Liver histology and quantification of triglyceride (TG) content in control and LBmal1KO mice (6 months on HFD). (E) Quantification of hepatic triglyceride (TG) content in control and LBmal1KO mice (6 months on HFD, n=7-8/genotype). (F) Hepatic TG content in control (adGFP) versus transient *Bmal1* over-expression (adBmal1) mice (n=5-6/group, 4 months on HFD). Liver samples were collected two weeks after tail vein injection of adenovirous. (G) Oxidative damage assessed by levels of protein carbonylation in liver lysate from HFD fed WT and LBmal1KO mice (showing 4 individual samples) with control (adGFP) or Fis1 over-expression adenovirus (adFis1) using Western blotting. C: negative control liver lysate from a WT mouse omitting DNPH substrates. Quantification normalized to Hsp60 is shown in Figure 6L. Samples were processed together and ran in two separate gels (indicated with the dotted line) in the same gel box. Subsequent Western blot procedures (transfer, antibody incubation, and signal development) were conducted in the same apparatus. Data presented as mean ± SEM. *p<0.05.

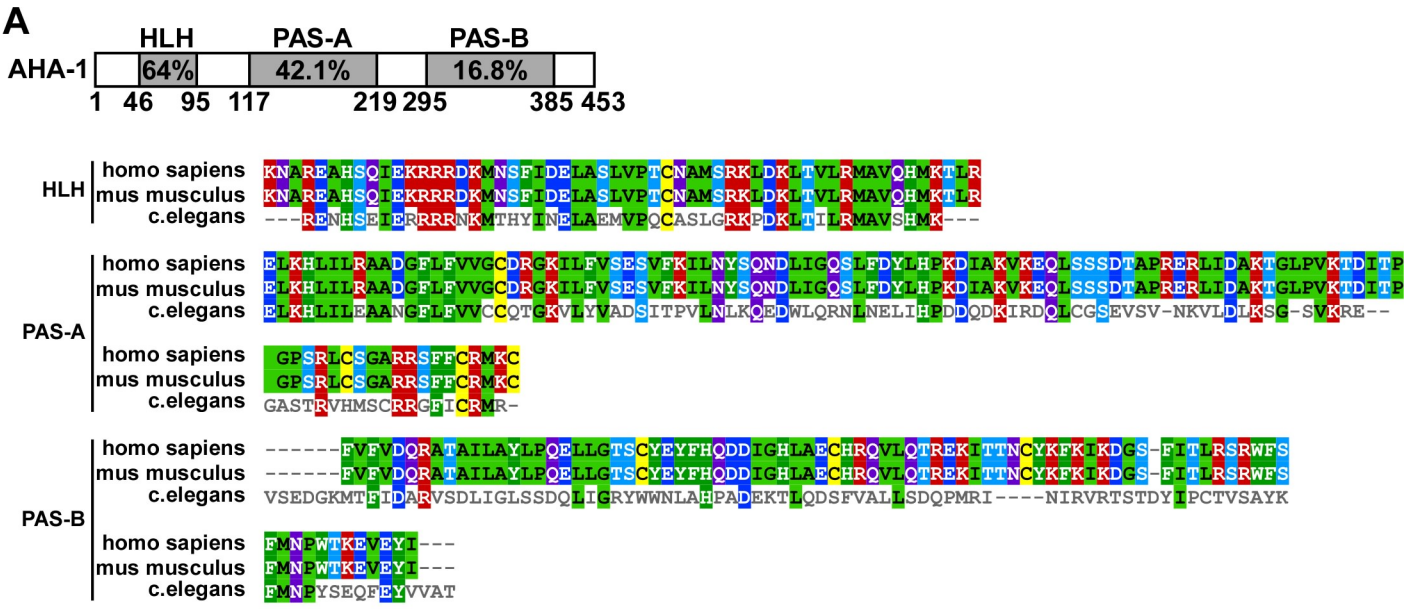

Compared proteins		Score (Bits)*	Identical residues	Including conservative substitutions	Gaps
Bmal1	Bmal2	489	274/559(49%)	362/559(64%)	44/559(7%)
Bmal1	aha-1	220	138/405(34%)	228/405(56%)	36/405(8%)
Bmal2	aha-1	184	113/369(31%)	188/369(50%)	32/369(8%)
Npas2	Npas4	52.4	70/327(21%)	124/327(37%)	37/327(11%)
Npas2	cky-1	72.4	83/330(25%)	147/330(44%)	27/330(8%)
Npas4	cky-1	195	112/325(34%)	176/325(54%)	45/325(13%)

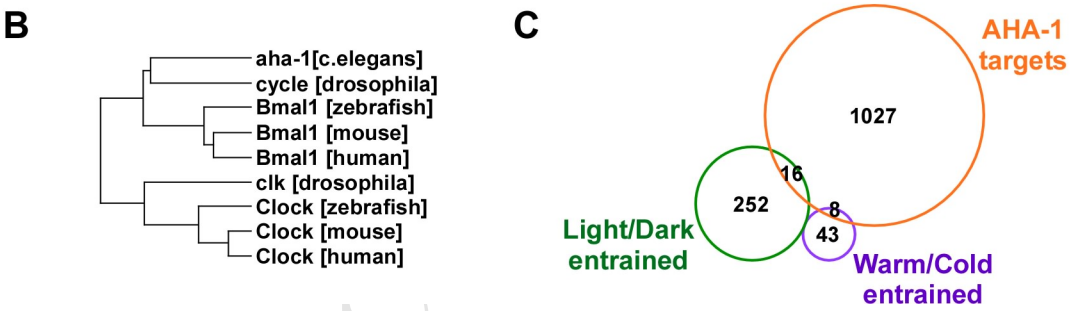

Figure S6 (related to Figure 7). AHA-1 is a Bmal1-like protein in *C. elegans*

(A) Sequence homology and alignment of helix-loop-helix (bHLH) and Per-Arnt-Sim (PAS) domains between *C. elegans* AHA-1 and mouse and human Bmal1. Bottom table: Sequence homology comparison between mouse Bmal1, Bmal2, Npas2, and Npas4 and worm AHA-1 and cky-1 (potential homologue of Npas4) using Ortho DB. *C. elegans* lacks Clock homologue. *A higher score indicates higher homology. (B) Phylogenetic analysis of mammalian *Bmal1* and worm *aha-1*. (C) Venn diagrams showing cross-comparison of light entrained, temperature entrained and AHA-1 regulated genes. Data derived from public sources (Gerstein et al., 2010; van der Linden et al., 2010)

SUPPLEMENTAL TABLES

The following Tables are in separate Excel files:

Table S1 (related to Figures 5 and S4). List of 211 and 122 Bmal1 target genes in mitochondrial function identified by (Koike et al., 2012) and by (Rey et al., 2011)

Table S3 (related to Figure 7). List of AHA-1 target genes in mitochondrial function based on analyses of ChIP-seq data derived from the ModEncode project

Table S2. Metabolic parameters of high fat feeding studies related to Figure 6

A. WT versus LBmal1KO

	WT	**LBmal1KO**
Body weight (g)	38.4 ± 1.3	49.1 ± 4.7*
WAT/body weight (%)	6.2 ± 0.1	6.9 ± 0.1
Liver/body weight (%)	3.8 ± 0.1	4.1 ± 0.1
Triglycerides (mg/dL)	30.3 ± 2.0	55.7 ± 4.7*
FFA (mmol/L)	0.34 ± 0.02	0.48 ± 0.04*
Cholesterol (mg/dL)	140.7 ± 9.0	184.8 ± 8.1*
Glucose (mg/dL)#	128.8 ± 5.1	167.6 ± 11.6*
Glucose (mg/dL)	190.4 ± 8.9	173.7 ± 8.9
Insulin (ng/mL)	0.69 ± 0.22	1.58 ± 0.29*
Food intake daytime (g)	1.01 ± 0.18	1.04 ± 0.15
Food intake nighttime (g)	1.98 ± 0.38	2.19 ± 0.44
Activity daytime (counts)	9075 ± 1433	7797 ± 813
Activity nighttime (counts)	26210 ± 321	25325 ± 1295

Fasted for 6 hours (n=7-8); 6 months on high fat diet. Data presented as mean ± SEM. *p<0.05. #Overnight fasted.

B. adGFP versus adBmal1

	AdGFP	AdBmal1
Body weight (g)	37.9 ± 0.9	35.6 ± 1.3
WAT/body weight (%)	5.7 ± 0.5	5.0 ± 0.7
Liver/body weight (%)	4.9 ± 0.3	6.1 ± 0.2
Triglycerides (mg/dL)	25.4 ± 1.0	25.1 ± 2.4
FFA (mmol/L)	0.31 ± 0.01	0.34 ± 0.03
Glucose (mg/dL)	194.0 ± 20.7	143.3 ± 6.8*
Insulin (ng/mL)	3.93 ± 1.06	1.57 ± 0.27*

Fasted for 6 hours (n=5-6); 4 months on high fat diet. Data presented as mean ± SEM. *p<0.05.

C. adGFP versus adFis1

	WT AdGFP	WT AdFis1	LBmal1KO AdGFP	LBmal1KO AdFis1
Body weight (g)	39.7 ± 2.9	37.2 ± 1.8	46.6 ± 2.8	41.6 ± 3.5
Liver/body weight (%)	5.2 ± 0.3	5.6 ± 0.3	6.21 ± 0.3	5.0 ± 0.3

Fasted for 6 hours (n=6); 6 months on high fat diet. Data presented as mean ± SEM.

Table S4. List of mouse cohorts related to Figures 1, 2, 4, 6, S1, S2, S4, and S5

Cohort info	No. Cohort	Age	Sex	Strain	Animal No.
adCRE vs adGFP	1*	8-10 weeks	Female**	C57BL/6J	4-5/genotype
adBmal1 vs adGFP	1*	10 weeks	Male	C57BL/6J	5/group
LBmal1KO vs WT, ad lib circadian study	1	10-12 weeks	Female**	C57BL/6J	3-4/genotype/time point
LBmal1KO vs WT, EM	2	8-10 weeks	Male	C57BL/6J	3/genotype/time point
LBmal1KO vs WT, fasted circadian study	1	10-12 weeks	Male	C57BL/6J	3-4/genotype/time point
LBmal1KO vs WT, high fat diet	2	38-40 weeks	Male	C57BL/6J	7-8/genotype
adBmal1 vs adGFP, high fat diet	1*	28 weeks	Male	C57BL/6J	5-6/group
LBmal1KO vs WT (with adFis1 or adGFP), high fat diet	1	32 weeks	Male	C57BL/6J	6/genotype
WT, high fat diet	1	28 weeks	Males	C57BL/6J	3/time point (Fig. S1A)

*Results were reproduced in separate cohorts.
**Similar results were obtained from male mice.

Table S5. List of primer sequences related to Figures 1, 5, 6, 7, S2, S4, and S5

RT-qPCR

Genes	Forward Sequence	Reverse Sequence	Accession Number
Aco2	GCCATGAGCCATTTTGAGCC	GTTCAACCGTTTACGGACAATG	NM_080633.2
Atp5a1	TCTCCATGCCTCTAACACTCG	CCAGGTCAACAGACGTGTCAG	NM_007505.2
Atp5sl	CGCAGTGAAGTTTCAGGACAAG	CCACAGGCACATTCTGGAAC	NM_025504.4
Bmal1	CACCGTGCTAAGGATGGCTG	CTGCTGCCCTGAGAATTAGG	NM_007489.4
Bnip3	CTCCCAGACACCACAAGATAC	CTTCCTCAGACAGAGTGCTG	NM_009760.4
Cox6c	GCTGCCTATAAGTTTGGCGTG	GCACTCTGAAAGATACCAGCC	NM_053071.2
Cpt1a	GGAGAGAATTTCATCCACTTCCA	CTTCCCAAAGCGGTGTGAGT	NM_013495.2
Crat	ATCCTGCCCAAGCAGGACTTTG	CGATGAGTTTGGCAGCAAACCG	NM_007760.3
mt-Co3	TTGAAACACCTGATGCTAGAAGTACT	AGCCTCGTACCAACACATGATGATCT	NC_005089.1
Dnm1l (Drp1)	CGTGACAAATGAAATGGTGC	CATTAGCCCACAGGCATCAG	NM_001276341.1
Ecsit	CTCAACATGACAGCGTCCAG	GCTACAGTAAGGTCCTGTCTAC	NM_012029.2
Fis1	AGGCTCTAAAGTATGTGCGAGG	GGCCTTATCAATCAGGCGTTC	NM_025562.3
Gpx1	CACCGAGATGAACGATCTGC	CATTCTCCTGGTGTCCGAACTG	NM_008160.6
Idh3a	GCTGCCAAAGCACCTATTCAG	GGGTCTTTAGTGGGCCTTTC	NM_029573.2
Mfn1	CCTACTGCTCCTTCTAACCCA	AGGGACGCCAATCCTGTGA	NM_024200.4
Mfn2	AGAACTGGACCCGGTTACCA	CACTTCGCTGATACCCCTGA	NM_001285920.1
mt-Nd1	AATCGCCATAGCCTTCCTAA	GCGTCTGCAAATGGTTGTAA	NC_005089.1
Ndufab1	CAGTTTGGACCAAGTGGAAATTATT	TGGACACATTAACTTCTCTGCATCT	NM_028177.3
Ndufa6	CGGTGAAGCCCATTTTCAGTC	GCATTAAGTGCACGGTGTTCG	NM_025987.3
Ndufaf4	CCGGAGTCAGTATCCAGAAATC	CCTTTGGTTCTTGTCGTGGTTC	NM_026742.4
Opa1	CTGAGGCCCTTCTCTTGTTAGG	CTGACACCTTCCTGTAATGCTTG	NM_001199177.1
Pdhb	AGTTGCCCAGTATGACGGTG	TCTGAGATGGGGGTGTCGAT	NM_024221.3
Pink1	CTGAGATGCCTGAGTCGGTG	GTGCAGACGGTCTCTTGCTG	NM_026880.2
Uqcrc1	AGACCCAGGTCAGCATCTTG	GCCGATTCTTTGTTCCCTTGA	NM_025407.2
Uqcrq	TTCAGCAAAGGCATCCCCAA	TAGACCACTACAAACGGCGG	NM_025352.2
C. elegans			
aha-1	TGGATCCATGGCAATCGGC	TCGAGCATATTTTCCAGATGGC	NM_001264398.1
atp-2	TCCGCCTCAGCTCAAACAAT	GATGACAGCGACAATGCGTC	NM_065710.5
atp-3	CCCAAGCAAGCCTCTTTACC	GTCTTCACCAGCTGAGCCTT	NM_001026250.4
cco-1	TGGATGCATGTGTGAGCAAG	CGACTCCCTTGAACCAGTGT	NM_060200.3
cco-2	AGTGGCCCGCTGATAAGTTC	GCAACTCGGAGAGAGCCTTT	NM_067280.5
mev-1	AGATCGTCGATTTCCCGCTC	AGCGCTGCTTCAACAGGTAT	NM_066882.5
nduf-7	TCGCTGCGCCAAGATATGAT	GGTTACTGTACCGGCAACGA	NM_060044.4
nuo-1	CCACGTCTGAAGCCTCCATT	TGTTGGAGCCACAGCTACAG	NM_063975.3
sdhb-1	CCTTCACCGTATGCACGACT	TGGCCTTAGCTGGGTTCAAG	NM_063591.6

shRNA

Gene	Sequence	Accession Number
Bmal1	CCCTCATGGAAGGTTAGAATA	NM_007489.4
Cry1	GCAAGCAGACTGAATATTGAA	NM_007771.3
Cry2	GCTCAACATTGAACGAATGAA	NM_009963
Per1	GGAGCATATCACATCCGAATA	NM_011065.4
Per2	AGTGATCGAGGACTAAGAAAT	NM_011066.3

SUPPLEMENTAL EXPERIMENTAL PROCEDURES

Animal studies

For circadian/diurnal studies mice between 8-12 weeks old were sacrificed every 4 hours starting at ZT4 for 24 hours with free access to food and water. For Figure S1A, mice on chow diet (12 weeks old male, n=3) or high fat diet for 5 months (28 weeks old, n=3) were sacrificed at ZT8 (fasted) and ZT20 (fed) for liver tissue collection. For constant fasting experiments, mice were sacrificed every 6 hours starting at ZT0 for 24 hours. Food intake and activities were measured using metabolic cages (Columbus Instruments). Glucose and insulin tolerance tests were performed on overnight fasted animals. For *in vivo* insulin signaling, 5 U/kg insulin was infused through the portal vein. Tissue samples were excised before and 5 min after insulin infusion. Serum lipids were determined at multiple time points from *ad lib* fed mice (Figure S5B) or from overnight fasted mice (Table S2).

Generation of stable Hepa 1-6 mouse hepatoma lines

Small hairpin RNA sequences against mouse *Bmal1*, *Cry1/2*, and *Per1/2* were obtained from the Decipher project [http://www.decipherproject.net] (Table S5). They were cloned into the pSIREN-RetroQ vector. Retroviral particles were generated through transient transfection of retroviral vectors into Phoenix packaging cell line. Supernatants were harvested two days after transfection. Hepa1-6 cells were infected with retroviral particles and selected against puromycin. For *in vitro* synchronization, 100 nM dexamethasone was applied to Hepa 1-6 cells for 1 hour. After thorough washing, fresh culture medium was added and cells were collected at the indicated time after dexamethasone removal.

Isolation of hepatocytes and liver mitochondria for bioenergetics assays

Primary hepatocytes were isolated from anesthetized animals perfused with a collagenase solution (Liberase TM, Roche) *in situ* through the portal vein (Liu et al., 2013). Cells were liberated into DMEM after perfusion. A 45% Percoll gradient was used to separate live and dead hepatocytes. For liver mitochondria collection, small

pieces of liver were rinsed in ice-cold mitochondrial isolation buffer (70 mM sucrose, 210 mM mannitol, 5 mM HEPES, 1 mM EGTA, and 0.2% fatty acid free BSA. pH=7.2) and homogenized in ~10 fold volume of the isolation buffer. The homogenates were spun down at 800 g for 10 minutes. The pellet was discarded and the supernatant was collected for additional two rounds of centrifugation at 8000 g for 10 minutes each. The resulting pellet fraction of each centrifugation contains the crude mitochondria. The pellets were resuspended in 100 μL of the isolation buffer and the protein quantities were determined.

Bioenergetics analyses

The oxygen consumption rate was determined on a XF24 or XFe24 Seahorse extracellular flux analyzer. For primary hepatocytes, freshly isolated cells in unbuffered glucose free DMEM (pH 7.4) supplemented with 10 mM pyruvate were plated in assay plates at 10^5 cells/well. Cells were allowed to attach in a CO_2 free incubator for 30 minutes. Stocks of respiratory inhibitors were loaded onto the analyzer for sequential injection of oligomycin (2 μM), FCCP (1 μM), and Rotenone (1 μM)/Antimycin (1 μM). For Hepa 1-6 cells, 50000 cells were plated in the assay plate to allow attachment overnight. At the day of experiment, culture media was exchanged with unbuffered, glucose free DMEM (pH 7.4) supplemented with 10 mM pyruvate. Similar procedures were carried out for primary hepatocytes, except for the FCCP concentration (0.5 μM). For mitochondrial coupling assays, isolated mitochondria were incubated in an initial buffer (mitochondrial assay buffer: 70 mM sucrose, 220 mM mannitol, 10 mM KH_2PO_4, 5 mM $MgCl_2$, 2 mM HEPES, 1 mM EGTA, and 0.2% fatty acid free BSA, pH 7.2) containing 10 mM succinate and 2 μM rotenone to determine uncoupled respiration. Sequential addition of 4 mM ADP, 2 $\mu g \cdot mL^{-1}$ oligomycin, 4 μM FCCP, and 4 μM antimycin A were used to determine state 3 and state 4 respiration. For electron flow experiment, an initial buffer containing 10 mM pyruvate/2 mM malate with 4 μM FCCP was used to determine electron flow starting from complex I. Subsequent additions of 2 μM rotenone, 10 mM succinate, 4 μM antimycin A, and 100 μM TMPD/10 mM ascorbate determine electron flow through complex II and complex IV, respectively. For coupling and electron flow assays, 25 μg mitochondrial protein was used.

Electron microscopy

Electron microscopy was conducted at Harvard Medical School Cell Biology Department. Following heart perfusion of 15 mL 2% paraformaldehyde, 2.5% glutaraldehyde in 0.1 M Na cacodylate HCl buffer (pH 7.3), small liver blocks were excised from the left lobe and placed in the same fixative at 4°C for 24 h. The blocks were postfixed with 1% OsO4/1.5% KFeCN6 for 2 hours, washed in water, and incubated in 1% aqueous uranyl acetate for 1 h, followed by dehydration through 50%, 70%, 90%, and 100% ethanol. Samples were embedded in TAAB and polymerized at 60°C for 48 h. Ultrathin sections (60 nm) were cut on a Reichert Ultracut-S microtome, stained with lead citrate and examined in a JEOL 1200EX Transmission electron microscope. Images were recorded with an AMT 2k CCD camera. To determine the location of hepatocytes relative to the liver lobules, additional sections were cut at 0.5 μm and stained with toluidine blue. Photographs were taken at 5000X magnification for 8 fields/liver, 70-80 μm from the centrilobular vein. Individual mitochondria were manually delineated using ImageJ software for determination of mitochondrial surface, density (number of mitochondria/surface area), and coverage (total mitochondrial surface/total cellular surface area). Only mitochondria that had a completely visible perimeter were counted. For each mouse, the total liver cell surface evaluated was 960 μm^2 (8 fields of 120 μm^2 each).

***C. elegans* studies**

Worms were maintained at 20°C on a growth media with OP50-1 bacteria (Mair et al., 2011). For RNAi experiments, media was supplemented with 100 $\mu g \cdot mL^{-1}$ carbenicillin and HT115 bacteria with an empty pL4440 vector (control) or HT115 expressing double-stranded RNA (dsRNA) of *aha-1*, obtained from the Ahringer RNAi library. Bacterial dsRNA expression was induced by 100 μL of 100 mM IPTG before transferring worms to the plate. RNAi feeding was carried out for 2 generations to enhance *aha-1* knockdown. For Lifespan analysis, worms were synchronized by picking gravid adults to fresh bacterial lawns and allowing egg laying to occur for 5 hours. The eggs were grown to day 1 adults and transferred to fresh lawns, which corresponded to time zero of the lifespan. Nematodes were transferred to fresh plates every 2-3 days until day 10 of adulthood and scored for survival by light head tapping every 1-2 days. Nematodes were censored for

non-age related deaths including crawling off the media, hatching of larvae inside adults and vulval ruptures. For lifespans in the UL1606 strain, day 1 adults of each strain were transferred to media supplemented with 100 µL of 1 mg·mL^{-1} FUDR (Sigma) to prevent hatching of embryos inside adults. In these experiments, nematodes were transferred again to fresh plates without FUDR on day 8 after egg laying had ceased. The log-rank Mantel-Cox test was used for statistical analysis. To visualize mitochondrial network, mitochondrial reporter worms were anaesthetized for 15 minutes in 0.2 mg·mL^{-1} tetramisole (Sigma) and mounted on a glass slide between a 2% agarose pad and glass coverslip. Body wall muscle of 10-30 L4/young adults were imaged at 40x and 63x with a Zeiss Axio Imager, Axiocam and ApoTome optical sectioning.

Public data analysis

Bmal1, Clock, and Cry1 bound genes were obtained from the published liver Bmal1, Clock, and Cry1 Chip-seq data (Koike et al., 2012). Koike's study showed 211 mitochondrial-related genes (out of 3,926 Bmal1 bound genes or of 2,499 Bmal/Cry/Clock bound genes), whereas 122 mitochondrial function related genes (out of 2,049 Bmal1 bound genes) were identified by (Rey et al., 2011). To visualize Chip-seq peaks in UCSC genome browser, aligned reads reported by the original publication were downloaded from GEO (http://www.ncbi.nlm.nih.gov/geo/) and processed using Homer (Heinz et al., 2010). The circadian phase of each transcription factor binding was calculated by JTK cycle (Hughes et al., 2010). The high-resolution circadian gene expression profiling in the liver was downloaded from GEO (GSE11923). The light and temperature entrainable genes in *C. elegans* were from published data (van der Linden et al., 2010). Chip-seq data of *C. elegans* AHA-1 at L4 stage was obtained from the ModEncode project (Celniker et al., 2009; Gerstein et al., 2010). The original peak calls were used for peak annotation by Homer. Gene ontology analyses were performed using DAVID [http://david.abcc.ncifcrf.gov].

SUPPLEMENTAL REFERENCES

Celniker, S.E., Dillon, L.A., Gerstein, M.B., Gunsalus, K.C., Henikoff, S., Karpen, G.H., Kellis, M., Lai, E.C., Lieb, J.D., MacAlpine, D.M., *et al*. (2009). Unlocking the secrets of the genome. Nature *459*, 927-930.

Gerstein, M.B., Lu, Z.J., Van Nostrand, E.L., Cheng, C., Arshinoff, B.I., Liu, T., Yip, K.Y., Robilotto, R., Rechtsteiner, A., Ikegami, K., *et al*. (2010). Integrative analysis of the Caenorhabditis elegans genome by the modENCODE project. Science *330*, 1775-1787.

Heinz, S., Benner, C., Spann, N., Bertolino, E., Lin, Y.C., Laslo, P., Cheng, J.X., Murre, C., Singh, H., and Glass, C.K. (2010). Simple combinations of lineage-determining transcription factors prime cis-regulatory elements required for macrophage and B cell identities. Mol. Cell *38*, 576-589.

Hughes, M.E., Hogenesch, J.B., and Kornacker, K. (2010). JTK_CYCLE: an efficient nonparametric algorithm for detecting rhythmic components in genome-scale data sets. J. Biol. Rhythms *25*, 372-380.

Koike, N., Yoo, S.H., Huang, H.C., Kumar, V., Lee, C., Kim, T.K., and Takahashi, J.S. (2012). Transcriptional architecture and chromatin landscape of the core circadian clock in mammals. Science *338*, 349-354.

Liu, S., Brown, J.D., Stanya, K.J., Homan, E., Leidl, M., Inouye, K., Bhargava, P., Gangl, M.R., Dai, L., Hatano, B., *et al*. (2013). A diurnal serum lipid integrates hepatic lipogenesis and peripheral fatty acid use. Nature *502*, 550-554.

Mair, W., Morantte, I., Rodrigues, A.P., Manning, G., Montminy, M., Shaw, R.J., and Dillin, A. (2011). Lifespan extension induced by AMPK and calcineurin is mediated by CRTC-1 and CREB. Nature *470*, 404-408.

Rey, G., Cesbron, F., Rougemont, J., Reinke, H., Brunner, M., and Naef, F. (2011). Genome-wide and phase-specific DNA-binding rhythms of BMAL1 control circadian output functions in mouse liver. PLoS Biol 9, e1000595.

van der Linden, A.M., Beverly, M., Kadener, S., Rodriguez, J., Wasserman, S., Rosbash, M., and Sengupta, P. (2010). Genome-wide analysis of light- and temperature-entrained circadian transcripts in Caenorhabditis elegans. PLoS Biol 8, e1000503.

Supplemental Table S1

Click here to download Supplemental Movies & Spreadsheets: Table S1 related to Figures 5 & S4.xlsx

Supplemental Table S3

Click here to download Supplemental Movies & Spreadsheets: Table S3 related to Figure 7.xlsx